A unifying and rigorous Shape From Shading method adapted to realistic data and applications

Emmanuel Prados (eprados@cs.ucla.edu)
UCLA Vision Lab. (USA)

Fabio Camilli (camilli@ing.univaq.it)
Dipartimento di Matematica Pura e Applicata
Università dell'Aquila (Italy)

Olivier Faugeras (Olivier.Faugeras@sophia.inria.fr)
Odyssée Lab. - INRIA Sophia Antipolis (France)

Abstract. We propose a new method for the Lambertian Shape From Shading (SFS) problem based on the notion of Crandall-Lions viscosity solution. This method has the advantage of requiring the knowledge of the solution (the surface to be reconstructed) only on some part of the boundary and/or of the singular set (the set of the points at maximal intensity). Moreover it unifies in an unique mathematical formulation the works of Rouy et al. [50, 34], Falcone et al. [21], Prados et al. [49, 46, 48], based on the notion of viscosity solutions and the work of Dupuis and Oliensis [17] dealing with classical solutions and value functions. Also, it allows to generalize their results to the "perspective SFS" problem recently simultaneously introduced in [46, 55, 13].

While the theoretical part has been developed in [44], in this paper we give some stability results and we describe numerical schemes for the SFS based on this method. We construct provably convergent and robust algorithms. Finally, we apply our SFS method to real images and we suggest some real-life applications.

Keywords: Shape From Shading, Hamilton-Jacobi equations, viscosity solutions, states constraints, finite differences.

1 Introduction

Shape From Shading (SFS) has been a central problem in the field of computer vision since the early days. The problem is to compute the three-dimensional shape of a surface from a black and white bi-dimensional image of that surface. The work in this field was pioneered by Horn who was the first to pose the problem as that of finding the solution of a nonlinear first-order Partial Differential Equation (PDE) called the brightness equation [26]. From this work, a number of various PDE based methods have been proposed; see for example [6, 16, 50, 29, 22, 30, 49] amongst others, and the overview papers [25, 31, 61, 19, 42].

The application of the partial differential equations theory to the Shape From Shading problem has been hampered by several difficulties. The first type arises from the simplification introduced in the modeling: orthographic cameras looking at Lambertian objects with a single point light source at infinity is the set of usual assumptions [61, 25]. The second type is mathematical: characterizing the solutions of the corresponding PDE has turned out to be a very difficult problem [50, 49]. The third type is algorithmic: assuming that the existence of a solution has been proved, coming up with provably convergent numerical schemes has turned out to be quite involved [20].

Concerning the mathematical aspects of the

problem, a breakthrough was made by Lions, Rouy and Tourin [50, 34] in the 90s by applying the notion of *continuous* viscosity solution. The theory of viscosity solutions offers simple and general theorems of existence and uniqueness for exactly the type of PDEs that arise in the context of SFS. In particular the theory allows to prove that, given a particular Dirichlet condition on the image boundary (verifying a compatibility condition), if the set of *critical points* (i.e. points x s.t. the intensity $I(x)$ is equal to 1; see section 2) is empty, then there exists an unique continuous viscosity solution satisfying the boundary conditions.

Unluckily two drawbacks limit the applicability of the continuous viscosity solution theory to SFS problems: the compatibility condition necessary for the existence of a solution and the loss of uniqueness of solution in presence of critical points [33].

Concerning the first point, consider for example the equation

$$|\nabla u(x)| = 1 \text{ for all } x \text{ in }]0,1[\qquad (1)$$

with $u(0) = u(1) = 0$. In this case the problem does not have a classical solution but has a continuous viscosity solution (see Figure 1-a)). The same equation (1) with $u(0) = 0$, $u(1) = 1.5$ does not have continuous viscosity solution. Now

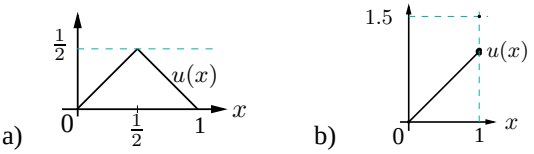

Figure 1: *a) Continuous viscosity solution of (1) with $u(0) = u(1) = 0$; b) discontinuous viscosity solution of (1) with $u(0) = 0$ and $u(1) = 1.5$.*

let us suppose that we make a large error on the boundary condition when we compute a numerical solution of the SFS problems. If this error is too large then there do not exist continuous viscosity solutions. In this case one may wonder what the numerical algorithm of [50, 34] computes. In [49, 48], Prados et al. answer this question by proposing to use the more general idea of *discontinuous* viscosity solutions [1]. For example, equation (1) with $u(0) = 0$, $u(1) = 1.5$ has a discontinuous viscosity solution (see figure (1-b) and [45] for more details).

If the set of critical points is not empty there exists an infinite number of continuous viscosity solutions which are characterized by their values at the critical points. Note that this result is general and applies equally well to all the SFS models described in section 2 (see [45]). In practice this set is generally not empty; as a consequence the SFS problem is ill-posed and to compute a numerical approximation of a solution, Rouy et al. and Prados et al. [50, 49, 45] must assume that the values of the solutions are given at the image boundary and at the critical points. This is quite unrealistic, because such values are not known, and it is even more unsatisfactory since small errors on these values create undesirable crests, see Figure 2-b) or [49] for an example with a real image. Therefore we would like to characterize relevant solutions with a minimum of data. In the approach proposed by Falcone [7, 21], it is required to specify the values of the solution on the boundary of the image domain, but not at the critical points. In order to achieve this, he uses the notion of singular viscosity solutions developed by Camilli and Siconolfi [8, 9]. Despite its advantages, this approach is not really adapted to the SFS problem, see for example Figure 2-c). In this figure, the singular solution $u_{\max}$ associated to the image obtained from the original surface u shows a highly visible crest where the surface should be smooth. Moreover this approach still requires the compatibility condition on the boundary datum.

An alternative approach to viscosity solution theory was proposed by Oliensis and Dupuis [38, 39, 18, 17]. They characterize a C^1 solution of a SFS equation by specifying only its values at the critical points which are local minima[1]. In particular, they do not specify the values of the solution on the boundary of the image [17]. Also, they provide algorithms for approximating these solutions. A strong limitation to the application of this method is the well known fact that first order Hamilton-Jacobi equations do not generally have classical solutions; see [33, 2, 1]. Moreover, even if we make appropriate assumptions in order to guarantee the existence of a classical solution,

[1] In [17, 40], Oliensis and Dupuis also characterize some (very constrained) C^2 solutions without any boundary data (neither at the boundary of the image, nor at the critical points) and propose a "global" algorithm. Such C^2 solutions are also considered by Kimmel and Bruckstein who propose another "global" algorithm [28].

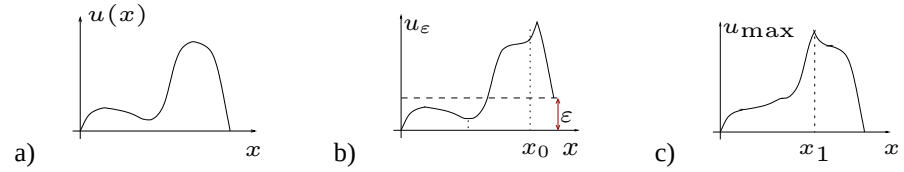

Figure 2: *a) original surface u; b) solution u_ε associated to corrupted boundary conditions and to the image obtained from the original surface a) with the Eikonal equation; c) maximal solution $u_{\max}$ (in Falcone's sense [7, 21]) associated to the same image. u_ε and $u_{\max}$ present a kink at x_0 and x_1.*

in practice, because of noise, of incorrect modeling, errors on parameters or on the depth values enforced at the critical points, the SFS equation really numerically solved may not have C^1 solutions.

Considering the drawbacks and the advantages of all these methods, it seems important to consider another class of weak solutions which extends the previous notions of viscosity solutions in such a way that the characterization of Dupuis and Oliensis still holds.
As we show in the second part of section 3.5.3 of [45] (see also [48, 42]), the notion of discontinuous viscosity solutions does not allow to impose the values of the solution at the critical points. Therefore, this notion cannot provide an extension of the Dupuis and Oliensis work. On the other side, the notion of singular viscosity solutions developed by Camilli and Siconolfi in [8, 9] uses Dirichlet conditions all around the boundary of the image and therefore it does not also provide a direct extension of the Dupuis and Oliensis work.
For such an extension, we must modify these notions and we must consider a "new" type of boundary conditions (called "state constraints" [53]). It turns out that the notion of viscosity solution for the SFS problem with the previous characteristics is the "Singular Discontinuous Viscosity Solution" (SDVS) with Dirichlet boundary conditions and state constraints we design and study here (a complete mathematical study of this notion can be found in [44, 43, 42]). The advantage of this notion is that it does not require a complete knowledge of the boundary data. We impose the Dirichlet condition on the part of boundary or of the singular set where we know the height of the surface, otherwise we "send" this datum to infinity, i.e. we impose a state constraint boundary condition. These solutions can be interpreted as maximal solutions and satisfy a comparison theorem.

Since in presence of critical points, discontinuous viscosity solutions are not unique, they do not satisfy stability properties. Oppositely, thanks to a comparison result, the SDVS is unique and is stable with respect to various perturbations of the SFS problem. For example it is stable with respect to smoothing effects or errors in the data, change of parameters in the model, numerical approximation. Moreover the notion of SDVS provides a mathematical framework unifying the work of Rouy et al. [34, 50], Prados et al. [49, 46], Falcone et al. [7, 21] and Dupuis and Oliensis [17].

This paper is the continuation of [48] in which we have proposed a rigorous method for the perspective and orthographic SFS problem, based on the notion of the *continuous* and *discontinuous* viscosity solutions. In [48], the mathematical study and the numerical computation of the solutions require the knowledge of the values of the solution all over the boundary of the image and at all "critical points". Because of this requirement, the experiments of [48] are limited to synthetic images. Here, we relax this restrictive and unrealistic assumption as much as possible. Also, we apply with success our method to real images and we can consider real-life applications.

The paper is organized as follows. We first review briefly the definition (Section 2-3) and the main existence and uniqueness properties of the SDVS (Section 4). These definitions and properties are completely described and demonstrated in the companion mathematical paper [44] (see also [43, 42]). Afterwards we complement [44] by explaining the state-constraints condition in illustrative and intuitive terms, by analyzing the relation between the SDVS and Dupuis-Oliensis solutions (Section 5-6) and by studying some additional stability properties (see Section 7). Section

8 is devoted to the numerical approximation of the SDVS. In Section 9, we prove that our method can be useful in a number of applications.

2 Hamiltonians for the Lambertian SFS problem

In this section, we recall various formulations of the SFS problem [48]. We deal with Lambertian scenes and suppose that the albedo is constant and equal to 1. Let Ω be the image domain. We represent the scene by a surface $\mathbf{S}$ which can be explicitly parameterized by using the function $S : \overline{\Omega} \to \mathbb{R}^3$:

$$\mathbf{S} = \left\{ S(x); \quad x \in \overline{\Omega} \right\}.$$

2.1 "Orthographic SFS"

This is the traditional setup for the SFS problem. We denote by $\mathbf{L} = (\alpha, \beta, \gamma)$ the unit vector representing the direction of the light source ($\gamma > 0$), $\mathbf{l} = (\alpha, \beta)$. The function S parameterizing the surface $\mathbf{S}$ is given by $S(x) = (x, u(x))$. The SFS problem is then, given I and $\mathbf{L}$, to find a function $u : \overline{\Omega} \longrightarrow \mathbb{R}$ satisfying the following brightness equation:

$$\forall x \in \Omega, \quad I(x) = \frac{-\nabla u(x) \cdot \mathbf{l} + \gamma}{\sqrt{1 + |\nabla u(x)|^2}},$$

This classical equation has been associated to various Hamiltonians:
1) In [50], Rouy and Tourin introduce

$$H^{orth}_{R/T}(x, p) = I(x)\sqrt{1 + |p|^2} + p \cdot \mathbf{l} - \gamma.$$

2) In [17], Dupuis and Oliensis consider

$$H^{orth}_{D/O}(x, p) = I(x)\sqrt{1 + |p|^2 - 2p \cdot \mathbf{l}} + p \cdot \mathbf{l} - 1.$$

3) In the case where $\mathbf{L} = (0, 0, 1)$, Lions et al. [34] deal with the Eikonal equation:

$$H^{orth}_{Eiko}(x, p) = |p| - \sqrt{\frac{1}{I(x)^2} - 1}.$$

2.2 "Perspective SFS"

First, let us assume that the scene is illuminated by a single point light source located at infinity. In [41, 46, 55, 13], the surface $\mathbf{S}$ is parameterized by $S(x) = u(x)\ (x, -\mathsf{f})$, where f represents the focal length. Combining the expression of $\mathbf{n}(x)$ and the change of variables $v = \log(u)$ (we assume that the surface is visible and below the camera, so $u > 0$), the following Hamiltonian follows from the irradiance equation:

$$H^{pers}_{P/F}(x, p) = I(x)\sqrt{\mathsf{f}^2|p|^2 + (x \cdot p + 1)^2} - (\mathsf{f}\,\mathbf{l} + \gamma x) \cdot p - \gamma.$$

See [48, 42], for more details.

Now, we assume that the light source is located at the optical center. This model corresponds nicely to the situation encountered in some medical protocols like endoscopy, in which the (point) light source is located very close to the camera, because of space constraints, see section 9.3 and [37, 23], for a SFS application in this area. This modeling also corresponds approximately to the situation encountered when we use a simple camera equipped with a flash; see sections 9.1 and 9.2 for two applications (face reconstruction and page restoration). In [48, 47], we parameterize the surface $\mathbf{S}$ by defining $S(x) = \frac{\mathsf{f}\, u(x)}{\sqrt{|x|^2 + \mathsf{f}^2}}\ (x, -\mathsf{f})$. Combining the expression of the normal vectors $\mathbf{n}(x)$, the expression of light source direction and the change of variables $v = \log(u)$, we obtain from the irradiance equation the following Hamiltonian:

$$H^{pers}_{F}(x, p) = I(x)\sqrt{\mathsf{f}^2|p|^2 + (p \cdot x)^2 + Q(x)^2} - Q(x),$$

where $Q(x) = \sqrt{\mathsf{f}^2/(|x|^2 + \mathsf{f}^2)}$. See [48, 42], for more details.

2.3 A generic Hamiltonian

In [48, 47], we prove that all the previous SFS Hamiltonians are special cases of the following "generic" Hamiltonian:

$$H_g(x, p) = \kappa_x \sqrt{|\mathbf{A}_x p + \mathbf{v}_x|^2 + K_x^2} + \mathbf{w}_x \cdot p + c_x,$$

with $\kappa_x, K_x \geq 0$, $c_x \in \mathbb{R}$, $\mathbf{v}_x, \mathbf{w}_x \in \mathbb{R}^2$ and $\mathbf{A}_x \in \mathbf{M}_2(\mathbb{R})$.
By using the Legendre transform (see appendix of

[42]), we rewrite this "generic" Hamiltonian as a supremum:

$$H_g(x,p) = \sup_{a \in \overline{B}_2(0,1)} \{-f_g(x,a)\cdot p - l_g(x,a)\}.$$

In [48, 42], we detail the exact expressions of f_g and l_g. This generic formulation considerably simplifies the analysis of the problem. In particular, this formulation unifies the orthographic and perspective SFS problems. Also, from a practical point of view, an unique algorithm can be used to numerically solve these various problems.

3 Singular Discontinuous Viscosity Solutions with Dirichlet Boundary Conditions and State Constraints

In this section we recall the definition of "Singular Discontinuous Viscosity Solution with Dirichlet boundary conditions and state constraints" (SDVS) we completely describe and study in [44, 43, 42].

Let Ω be a bounded open subset of $\mathbb{R}^N$ with smooth boundary (say $W^{2,\infty}$). In the SFS problem $N = 2$. So Ω is a smooth part of rectangular domain $]0, X[\times]0, Y[$ which typically represents the domain of definition of the image. We consider the Hamilton-Jacobi equation

$$H(x, \nabla u) = 0, \qquad \forall x \in \Omega, \tag{2}$$

where $H : \overline{\Omega} \times \mathbb{R}^N \to \mathbb{R}$, the Hamiltonian, is continuous in (x,p), convex and coercive ($\liminf_{|p|\to+\infty} H(x,p) = +\infty$, uniformly in $x \in \overline{\Omega}$) with respect with p. Moreover we assume that there exists a subsolution $\psi \in C^1(\Omega)\cap W^{1,\infty}(\Omega)$ of (2) (i.e: $\forall x \in \Omega,\ H(x, \nabla\psi(x)) \leq 0$) and for any $\lambda \in (0,1)$ and $p \in \mathbb{R}^N$ s.t $H(x,p) \leq 0$ and $p \neq \nabla\psi(x)$ then

$$H(x, \lambda p + (1-\lambda)\nabla\psi(x)) < 0. \tag{3}$$

We denote by $\mathcal{S}$ the set of *singular points* of H with respect to ψ :

$$\mathcal{S} = \{x \in \overline{\Omega} \mid H(x, \nabla\psi(x)) = 0\},$$

i.e. the set where ψ fails to be a strict subsolution of (2). $\mathcal{S}$ is closed by the continuity of $\nabla\psi$ and H. We recall that if $\mathcal{S}$ is empty then there exists an unique viscosity solution to (2) completed with an appropriate boundary condition. If $\mathcal{S}$ is not empty, then in general uniqueness fails. We assume that

$$\mathcal{S} \cap \partial\Omega = \emptyset. \tag{4}$$

With the exception of the coercivity condition, all the previous hypotheses hold for the various SFS Hamiltonians considered in section 2 (see [48, 42]) as soon as the intensity image I is continuous and verifies $I(x) > 0$ for any $x \in \overline{\Omega}$. The coercivity condition holds as long as the ambiguity cone (set of the normal vectors $\mathbf{n}$ verifying $\cos(\mathbf{n}, \mathbf{L}) = I(x)$) does not intersect the orthogonal plane to the projection line; see Figure 3.

In [48, 42], we prove that for all the SFS equations presented in section 2 the set of singular points $\mathcal{S}$ corresponds to the set of "critical points" $\{x \in \overline{\Omega} \mid I(x) = 1\}$ where I is the brightness image.

We complement (2) with a "boundary condition" which represents the part of the data of the surface to reconstruct that we have at our disposal. We consider a function $\varphi : \overline{\Omega} \to \mathbb{R} \cup \{+\infty\}$, $\varphi \not\equiv +\infty$, l.s.c. and continuous in $\{x \in \overline{\Omega} : \varphi(x) < +\infty\}$. Moreover we assume that the set $K = \{x \in \Omega : \varphi(x) < +\infty\}$ is a (possible empty) subset of Ω such that

$$\overline{K} \subset \Omega, \tag{5}$$

where $\overline{K}$ is the closure of K in $\mathbb{R}^N$. The set K represent the available data inside Ω.

With equation (2), we associate the "Dirichlet Boundary Conditions" (DBC)

$$u(x) = \varphi(x), \quad \forall x \in \overline{\Omega} \tag{6}$$

(of course, this constraint defined on the whole set $\overline{\Omega}$ must not be considered in pointwise sense).

At points $x \in \partial\Omega$ where $\varphi(x) = +\infty$, we say that we impose a *state constraint* boundary condition (see [53], [10]).

We first give the definition of viscosity subsolution, which coincides with the standard one in viscosity solution theory.

Definition 1 (Viscosity subsolution of (2)-(6)) *A locally bounded function u, u.s.c in $\overline{\Omega}$, is called a viscosity subsolution of (2)–(6) in $\overline{\Omega}$ if*

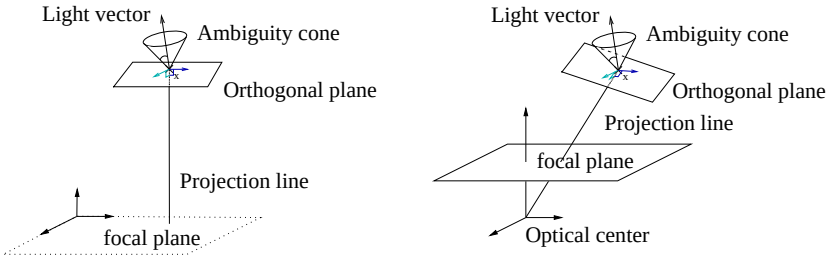

a) Orthographic case b) Perspective case

Figure 3: Ambiguity cone and plane orthogonal to the projection line.

i) *For any* $\Phi \in C^1(\Omega)$, *for any local maximum* $x_0 \in \Omega$ *of* $(u - \Phi)$ *in* Ω,

$$H(x_0, \nabla\Phi(x_0)) \leq 0$$

ii) $\circ$ $\forall x_0 \in K, \quad u(x_0) \leq \varphi(x_0)$.

$\circ$ $\forall x_0 \in \partial\Omega, \quad [u(x_0) \leq \varphi(x_0)]$ *or* $[\forall \Phi \in C^1(\overline{\Omega})$ *s.t.* x_0 *is a local maximum of* $(u - \Phi)$ *in* $\overline{\Omega}$, $H(x_0, \nabla\Phi(x_0)) \leq 0]$.

The regularity of $\partial\Omega$ and the hypotheses on H imply that a viscosity *subsolution of (2) is Lipschitz continuous in* Ω.

Before giving the definition of the singular viscosity supersolution of (2)-(6), we need to detail various preliminary definitions. Let $\mathcal{Z}(x)$ be the multivalued map on Ω defined as:

$$\mathcal{Z}(x) = \{p \in \mathbb{R}^N : H(x,p) \leq 0\}. \qquad (7)$$

By the assumptions on H, it follows that for any $x \in \overline{\Omega}$ the set $\mathcal{Z}(x)$ is compact, convex and strictly star-shaped with respect to $\nabla\psi(x)$ and

$$\partial\mathcal{Z}(x) = \{p \in \mathbb{R}^N \mid H(x,p) = 0\}. \qquad (8)$$

For all the SFS Hamiltonians, it is easy to see that

$$\mathcal{Z}(x) = \{\nabla\psi(x)\} \quad \text{for any } x \in \mathcal{S}. \qquad (9)$$

Remark: Under the hypothesis (9), the continuity of H provides a new characterization of $\mathcal{S}$: $x \in \mathcal{S} \Longleftrightarrow \mathcal{Z}(x) = \{\nabla\psi(x)\}$.

As explained in [9], (8) is a geometric property which allows us to study the equation $H(x, \nabla u) = 0$ through the level sets $\mathcal{Z}(x)$. Let W be an open subset of Ω. If $F(x,p)$ is any continuous function representing $\mathcal{Z}(x)$ in the sense that for all $x \in W$,

$$\begin{array}{ll} F(x,p) < 0 & \text{if and only if} \quad p \in Int(\mathcal{Z}(x)), \\ F(x,p) = 0 & \text{if and only if} \quad p \in \partial\mathcal{Z}(x), \end{array} \qquad (10)$$

then equation

$$F(x, \nabla u) = 0, \qquad \forall x \in W,$$

is equivalent to equation

$$H(x, \nabla u) = 0, \qquad \forall x \in W,$$

from the viscosity point of view.

The multiplicity of the classical viscosity solutions is due to the fact that the subsolution ψ fails to be strict at the points $x \in \mathcal{S}$. So, to get around this difficulty the main idea consists in transforming the equation $H(x, \nabla u) = 0$ in a new equation $F(x, \nabla u) = 0$ equivalent on $\Omega \setminus \mathcal{S}$ such that $\forall x \in \mathcal{S}$, $F(x, \nabla\psi(x)) < 0$ (i.e. ψ still is a strict subsolution on $\mathcal{S}$). To this end, let us introduce the gauge function $\rho(x,p)$ of $\mathcal{Z}(x)$; see [27, 8, 9]. We set for any $x \in \overline{\Omega}$, $p \in \mathbb{R}^N$,

$$\rho(x,p) = \inf\{\lambda > 0 : \lambda^{-1}p + (1 - \lambda^{-1})\nabla\psi(x) \in \mathcal{Z}(x)\}. \qquad (11)$$

As in [2], (see also Proposition 5.1 of [9]), we can prove that the function ρ is continuous in $(\overline{\Omega}\setminus\mathcal{S}) \times \mathbb{R}^N$ and verifies the homogeneity condition:

$$\begin{array}{l} \forall \mu > 0 \quad \text{and} \quad \forall (x,p) \in \overline{\Omega} \times \mathbb{R}^N, \\ \quad \rho(x, \mu p + (1 - \mu)\nabla\psi(x)) = \mu\rho(x,p). \end{array} \qquad (12)$$

Moreover, $p \in \mathcal{Z}(x)$ if and only if $\rho(x,p) \leq 1$. In particular, we can easily verify that for all x in $\Omega \setminus \mathcal{S}$,

$$\begin{array}{ll} \rho(x,p) < 1 & \text{if and only if} \quad p \in Int(\mathcal{Z}(x)), \\ \text{and} & \\ \rho(x,p) = 1 & \text{if and only if} \quad p \in \partial\mathcal{Z}(x). \end{array}$$

Then the equation

$$\rho(x, \nabla u(x)) - 1 = 0,$$

defines an equation equivalent to (2) in $\Omega \setminus \mathcal{S}$. Moreover, if $x \in \mathcal{S}$, we have $\rho(x, \nabla\psi(x)) = 0$; so $\rho(x, \nabla\psi(x)) - 1 < 0$.

Roughly speaking, the definition of the *classical* notion of viscosity supersolution is equivalent to *"There does not exist a subtangent which is also a strict subsolution"* (globally, we say that a function ϕ is a subtangent to u at x_0 if $\phi(x_0) = u(x_0)$ and $\phi \leq u$ on a neighborhood of x_0).
In other respects, if u is a classical viscosity solution of (2), we can prove (see for example [44, 42, 43]) that, on each regular[2] connected component $\mathcal{S}_i$ of $\mathcal{S}$, there exists c_i such that

$$\forall x \in \mathcal{S}_i, \;\; u(x) = \psi(x) + c_i.$$

So, if $x_0 \in Int(\mathcal{S}_i) \neq \emptyset$, then ψ is always a subtangent to u at x_0 and a strict subsolution of the new equation $\rho(x, \nabla u(x)) - 1 = 0$. If we want to adapt the previous definition for the singular points, we need to weaken the topology in such a way that all the neighborhoods of x_0 contain the whole subset $\mathcal{S}_i$. Thus ψ would be not systematically a subtangent.

Let us set, for any $x \in \overline{\Omega}$,

$$r(x) = \sup\{r > 0 \mid B(\nabla\psi(x), r) \subset \mathcal{Z}(x)\}.$$

By Lemma 3.1 in [9], it is proved that $r(x)$ is nonnegative and $r(x) = 0$ if and only if $x \in \mathcal{S}$. As in [8, 9], we proceed defining a semidistance on $\overline{\Omega}$. We set for any $x, y \in \overline{\Omega}$,

$$S(x,y) = \inf \Big\{ \int_0^1 r(\xi(t)) \mid \xi'(t)|dt \;\; : \\ \xi \in \; W^{1,\infty}_{([0,1],\overline{\Omega})} s.t.\; \xi(0) = x \text{ and } \xi(1) = y \Big\}. \tag{13}$$

S is a semidistance on $\overline{\Omega}$, but in general not a distance since, if $x_0 \in \mathcal{S}$, the set of points which have 0 S-distance from x_0 is in general a subset of $\mathcal{S}$ containing elements different from x_0. The family of balls:

$$B_S(x_0, R) = \{x \in \Omega \mid S(x_0, x) \leq R\}$$

induces a topology τ_S in Ω. Note that on a neighborhood of a point $x \in \Omega \setminus \mathcal{S}$ the topology τ_S is equivalent to the Euclidean topology. At a point $x \in \mathcal{S}$, it is a weaker topology. We denote by $B_S(x_0)$ the subset $B_S(x_0) = \{x \in \overline{\Omega} \mid S(x_0, x) = 0\}$.

Definition 2 *A Lipschitz-continuous function ϕ is said to be a strict subsolution of (2) in an open subset A of Ω if v is a viscosity subsolution of*

$$\rho(x, \nabla\phi) \leq \theta \qquad x \in A$$

for some $\theta \in \;]0, 1[$.

Definition 3 (Singular viscosity supersolution of (2)-(6)) *A locally bounded function $v : \overline{\Omega} \to \mathbb{R}$, l.s.c. on $\overline{\Omega}$, is called a singular viscosity supersolution of (2)-(6) if:*

i) For any $x_0 \in \Omega \setminus K$, it does not admit a S-subtangent at x_0 which is a strict subsolution of (2) in a neighborhood of $B_S(x_0)$

ii) For any $x_0 \in \partial\Omega \cup K$,

- *it does not admit a S-subtangent at x_0 which is a strict subsolution of (2) in a neighborhood of $B_S(x_0)$*
- or *there exists $x \in B_S(x_0)$ such that $v(x_0) \geq \varphi(x) + \psi(x_0) - \psi(x)$.*

Let us emphasize that, if the set $\mathcal{S} \cup K$ is empty, then the singular supersolutions of (2)-(6) coincide with the standard discontinuous viscosity supersolutions of (2)-(6). Let us also recall that, at the points $x_0 \in \partial\Omega$ where $\varphi(x_0) = +\infty$, the Dirichlet boundary condition corresponds with the classical state constraint condition [53, 10]. Now, we can give the definition of the singular viscosity solution of (2)-(6).

Definition 4 (Singular viscosity solution of (2)-(6)) *A continuous function $u : \overline{\Omega} \to \mathbb{R}$ is called a singular viscosity solution of (2)-(6) if it is a subsolution and a singular supersolution of (2)-(6).*

We will call "Singular Discontinuous Viscosity Solutions" (SDVS) with Dirichlet boundary conditions and state constraints , the singular solution of (2)-(6).

[2] In [8], a counterexample based on the classical Whitney's function shows that if $\mathcal{S}_i$ is not regular the previous property can be false.

4 Existence and uniqueness of SDVS

In this section we recall the main results we prove in [44, 42, 43]. We start with an existence result given by a representation formula for a SDVS of (2)-(6).

Let $\delta : \Omega \times \mathbb{R}^N \to \mathbb{R}$ be the support function of the set $\tilde{\mathcal{Z}}(x)$, i.e.:

$$\delta(x,p) = \max\{pq : q \in \tilde{\mathcal{Z}}(x)\}, \qquad (14)$$

where $\tilde{\mathcal{Z}}(x) = \mathcal{Z}(x) - \nabla\psi(x) \doteq \{y - \nabla\psi(x) \mid y \in \mathcal{Z}(x)\}$. The function $\delta(x,p)$ is continuous in $\Omega \times \mathbb{R}^N$, convex and positively homogeneous in p. We denote for any $x, y \in \overline{\Omega}$,

$$L(x,y) = \inf\{\textstyle\int_0^1 \delta(\xi(t), -\dot{\xi}(t))dt \mid \xi \in W^{1,\infty}_{([0,1],\overline{\Omega})} \text{ s.t. } \xi(0) = x \text{ and } \xi(1) = y\}. \qquad (15)$$

REMARK. If $x \in \mathcal{S}$, then $\tilde{\mathcal{Z}}(x) = \{0\}$ and therefore $\delta(x,p) = 0$ for any $p \in \mathbb{R}^N$. Also, the inverse statement holds. Hence

$$\delta(x,p) = 0 \quad \text{for any } p \in \mathbb{R}^N \iff x \in \mathcal{S} \iff r(x) = 0.$$

So for any $x, y \in \overline{\Omega}$,

$$L(x,y) = 0 \Longleftrightarrow S(x,y) = 0.$$

Theorem 1 (Existence) *The function*

$$V(x) = \psi(x) + \min\{\, L(x,y) + \varphi(y) - \psi(y) \mid y \in \partial\Omega \cup K \,\}. \qquad (16)$$

is a SDVS to (2)-(6).

Now, let us analyze the uniqueness of the SDVS. We assume that there exists a neighborhood A of $\partial\Omega$ and $\lambda > 0$ such that $\forall p, q \in \mathbb{R}^N$ and $\forall x \in A$

$$|H(x,p) - H(x,q)| \le \lambda |p - q|. \qquad (17)$$

In other words, we impose that H is Lipschitz continuous in p (with a Lipschitz constant which does not depend on $x \in A$) on a neighborhood of $\partial\Omega$. We have the following strong comparison result.

Theorem 2 (Uniqueness) *Let $u, v : \overline{\Omega} \to \mathbb{R}$ be respectively an u.s.c. subsolution of (2)-(6), and a l.s.c. singular supersolution of (2)-(6). Then*

$$\forall x \in \Omega, \quad u(x) \le v(x).$$

Let us note that clearly the strong uniqueness involves the uniqueness on Ω of the singular viscosity solution of (2)-(6): i.e, if u_1 and u_2 are two singular viscosity solutions of (2)-(6), then for any $x \in \Omega$, $u_1(x) = u_2(x)$. Moreover, it proves that this solution is continuous on Ω, therefore it is Lipschitz continuous on Ω (because subsolutions are Lipschitz continuous).

Note that all the SFS Hamiltonians H^*_{pers} and H^*_{orth} verify the hypothesis (17) (see [48, 42]). Also, we can prove easily that Theorems 1 and 2 apply for all the Shape From Shading equations described in section 2 (see [42, 43]). Consequently the SFS equations complemented by the constraint (6) have an unique SDVS.

5 A general framework for SFS

In this section, we explain *why the notion of state constraints is relevant* when we do not know the values of the solution and we describe this boundary condition in a more intuitive way. Moreover, we show that *the notion of SDVS provides a general mathematical framework unifying the previous mathematical frameworks* based on viscosity solution theory proposed in the SFS literature.

The main contribution of the notion of SDVS lies in the possibility to impose the heights of the solution at the singular points if we know them[3] and on the possibility to "send to infinity" the boundary conditions if we do not know them. This possibility also holds for all the points located on the boundary of the image $\partial\Omega$. Let us recall that in the previous work [50, 49, 46, 45, 7, 21], the various notions of viscosity solutions [continuous, discontinuous or singular] are used with (finite) Dirichlet conditions on the boundary of the images. Note that, in [34], Lions et al. have already

[3] This is impossible with discontinuous viscosity solutions; see the second part of section 3.5.3 of [45]. It is possible with continuous viscosity solutions but compatibility conditions are required. In [7, 21], Falcone et al. "send" systematically the singular points "at the infinity".

used the notion of states constraints, but they used it only to deal with apparent contours and in the eikonal setup. More precisely, they use it only at the points $x \in \partial\Omega$ such that $I(x) = 0$ and "$\frac{\partial u}{\partial n} = -\infty$". Here, we use the state constraints at each point of $\partial\Omega$, where we do not know the value of the solution. Also, let us remark that in [17], the authors implicitly impose state constraints.

Let us focus on the points on the *boundary $\partial\Omega$ of the image*. For simplicity, let us assume that we know the values of the solution at all the singular points. First, in contrast with the Dirichlet and Neumann boundary conditions, the state constraints are interesting because they do not require any data. Let us recall that the Dirichlet (respectively, Neumann) boundary conditions require the knowledge of the values of the solution (respectively, the values of $\nabla u(x) \cdot n(x)$, where $n(x)$ is the unit inward normal vector to $\partial\Omega$ at the point x) on the boundary of the domain. But, in general, we rarely have such data at our disposal. Second, the notion of state constraints is also interesting because it provides a relevant solution as soon as the image is yielded by a "surface" u which verifies the supersolution constraint on $\partial\Omega$. Also, as we explain below, this constraint is very weak and it is commonly verified with real observable surface. Recall that an equivalent way to define the viscosity supersolution constraint at a point $x \in \partial\Omega$ is to require that

$$H(x, \xi) \geq 0, \quad \forall \xi \in D^- u(x) \tag{18}$$

where

$$D^- u(x) = \left\{ \xi \in \mathbb{R}^N \mid \liminf_{y \to x, y \in \overline{\Omega}} \frac{u(y) - u(x) - \xi(y - x)}{|y - x|} \geq 0 \right\} \tag{19}$$

(see for example [2, 1, 10]). This constraint can be roughly interpreted as follows: *For all plan P subtangent to u at x, the gradient ∇P verifies* $H(x, \nabla P) \geq 0$. To better understand the constraint (18) for x in $\partial\Omega$, let us consider the particular case of a differentiable solution.

Proposition 1 *Let u be a solution differentiable on $\overline{\Omega}$ of the HJB equation associated with the Hamiltonian*

$$H(x, p) = \sup_{a \in A} \{-f(x, a).p - l(x, a)\}. \tag{20}$$

and denote by $a_0(u, x)$ the optimal control of (20) *associated to u at the point x (i.e. $a_0(u, x)$ is the control $a \in A$ maximizing $-f(x, a) \cdot \nabla u(x) - l(x, a)$). If for $x \in \partial\Omega$,*

$$f(x, a_0(u, x)) \cdot n(x) > 0, \tag{21}$$

where $n(x)$ is the unit inward *normal vector to $\partial\Omega$ at the point x, then* (18) *is satisfied.*

In other words, the surface u is a supersolution on $\partial\Omega$ (i.e. u verifies the state constraints on $\partial\Omega$) as soon as the *dynamic of the optimal control* (associated with u) *points inward of* Ω at all points x on the boundary $\partial\Omega$. In the classical *example of the Eikonal equation*, the optimal control associated to a differentiable function u is

$$f(x, a_0(u, x)) = -a_0(u, x) = -\frac{\nabla u(x)}{|\nabla u(x)|}.$$

So in this example, *u is a supersolution on $\partial\Omega$ as soon as* for all x on $\partial\Omega$, *the gradient $\nabla u(x)$ points outward of* Ω, i.e. roughly speaking, when $u(x)$ *"increases" when x come up to* $\partial\Omega$. More generally, (21) can be globally interpreted as "$u(x) - \psi(x)$ increases when x come up to $\partial\Omega$".
In other respects, let us note that proposition 1 shows that the notion of state constraints coincides with the constraint formulated by Dupuis and Oliensis in assumption 2.1 of [17] and introduced in the case of solutions C^1.

PROOF OF PROPOSITION 1. Let $x \in \partial\Omega$ be such that (21) is satisfied. We have for $c \leq 0$

$$\begin{aligned} &H(x, \nabla u(x) + cn(x)) = \\ &\quad H(x, \nabla u(x) + cn(x)) - H(x, \nabla u(x)) \geq \\ &- f(x, a_0(x, u)) \cdot (\nabla u(x) + cn(x)) - l(x, a_0(x, u)) \\ &\quad - (-f(x, a_0(x, u)) \cdot \nabla u(x) - l(x, a_0(x, u))) \\ &\qquad = -f(x, a_0(x, u)) \cdot cn(x) \geq 0. \end{aligned} \tag{22}$$

Moreover, since u is differentiable on $\overline{\Omega}$, we have

$$D^- u(x) = \{\xi \mid \xi = \nabla u(x) + cn(x),\ c \leq 0\}.$$

Thus, for any $\xi \in D^- u(x)$,

$$H(x, \xi) \geq 0.$$

So the constraint (18) holds. □

Now, *let us focus on the singular points*. We denote by Π_u the set of points in Ω such that a

constant function is S-subtangent to $u-\psi$ at x. If $x \notin \mathcal{S}$ or $B_S(x) = \{x\}$, this means that x is a local minimum point for $u-\psi$. For this reason we call Π_u the set of minimum points of $u-\psi$. We also set

$$\Gamma_u = \{x \in \Omega \mid \exists y \in B_S(x) \text{ verifying } u(x) \geq \varphi(y) + \psi(x) - \psi(y)\}. \quad (23)$$

Now, let us assume that $K \subset \mathcal{S}$. Here we are interested in fixing the values of the solution in a subset of the singular set.

Theorem 3 *Let u be a (discontinuous) viscosity solution of (2)-(6) such that $u(x) \leq \varphi(x)$ for any $x \in K$. If $\Pi_u \subset \Gamma_u$ then u is the SDVS of (2)-(6).*

In other words, the SDVS is the unique discontinuous viscosity solution u of (2)-(6) (verifying $\forall x \in K, u(x) \leq \varphi(x)$) without local minima on $\Omega \backslash \Gamma_u$. Of course, the reciprocal statement of Theorem 3 holds. That is to say that the SDVS cannot have points of local minimum (in Ω) outside of Γ_u. In effect, by contradiction, if $u-\psi$ admits a constant function S-subtangent to $x_0 \notin \Gamma_u$, then the function ψ is a S-subtangent to u at x_0. Since by the definition of $\mathcal{S}$, ψ is a strict subsolution of (2) it follows that u cannot be a (singular) supersolution at x_0.
An important interpretation and consequence of Theorem 3 is the following:

The (discontinuous) viscosity solutions of (2)-(6) can be characterized only by their minima.

That is to say, if u is a (discontinuous) viscosity solutions of (2)-(6) then u is the (unique) SDVS of

$$\begin{cases} H(x, \nabla u) = 0, & \forall x \in \Omega, \\ u(x) = \hat{\varphi}(x), & \forall x \in \partial\Omega \cup \mathcal{S}, \end{cases}$$

where

$$\hat{\varphi}(x) = \varphi(x), \quad \forall x \in \Pi_u \cup \partial\Omega,$$
$$\hat{\varphi}(x) = +\infty, \quad \forall x \in \mathcal{S} \setminus \Pi_u.$$

Thus this result extends the work of Dupuis and Oliensis [17]. In [17], Dupuis and Oliensis characterize the C^1 solutions by their values at the local minimum points[4]. Here, we have extended this characterization to the (discontinuous) viscosity solutions.

PROOF OF THEOREM 3. See [44, 42, 43]. □

Finally, let us emphasize that the notion of SDVS allows to *unify* the various theories based on viscosity solutions used for solving the SFS problem. In effect,

- in the case where the Dirichlet Boundary Conditions (DBC) are finite on $\partial\Omega \cup \mathcal{S}$ and the compatibility condition (see [33]) holds, then the SDVS of (2)-(6) is the continuous viscosity solution used by [50, 34, 49, 46];
- in the case where the DBC are finite on $\partial\Omega$ and where there do not exist singular points, then the SDVS of (2)-(6) coincides with the discontinuous viscosity solution used by [46, 45] (the compatibility conditions are no more required);
- when the DBC are finite on the boundary of the image and state constraints are imposed at the singular points, the SDVS of (2)-(6) corresponds to the Camilli and Siconolfi's singular viscosity solutions [8, 9] used by Falcone et al. [7, 21];
- as we have demonstrated above the SDVSs coincide with the C^1 solutions of (2) verifying the assumption 2.1 of Dupuis and Oliensis (when smooth solutions exist). Therefore, when there do not exist C^1 solutions, the notion of SDVS allows to extend the work of Dupuis and Oliensis [17].

As a consequence, all the theoretical results of Falcone et al. [7, 21], Rouy et al. [50, 34], Prados et al. [49] and Oliensis et al. [17] which only deal with "orthographic Shape From Shading", are *automatically extended to the "perspective SFS"* (use H_F^{pers} and $H_{P/F}^{pers}$).

6 Minimal and global viscosity solutions

The SDVS allows to send the boundary conditions to $+\infty$; thereby obtaining the "maximal" solution. So for obtaining the "minimal" solution, it can seem natural to send them to $-\infty$. Nevertheless

[4] Let us recall that in [17], the functional cost l had to be positive. This is why Dupuis and Oliensis need to introduce the SFS Hamiltonian $H_{D/O}^{orth}$ (instead of dealing with $H_{R/T}^{orth}$). Here, we relax this constrained assumption.

with such boundary conditions there do not exist solutions. In other respects, the viscosity solutions of the equation $H(x, \nabla u) = 0$ are different from the viscosity solutions of $-H(x, \nabla u) = 0$. For example, the opposite two equations on $]0, 1[$ associated with $H_1(x, p) = |p| - 1$ constrained by $u(0) = u(1) = 0$ have an unique viscosity solution given by Figure 4. By schematizing, the solution of $H(x, \nabla u) = 0$ allows upward kinks whereas $-H(x, \nabla u) = 0$ allows downward kinks. Moreover, it is well known that:

$$[u \text{ solution of } -H(x,p)] \iff [-u \text{ solution of } H(x,-p)]. \quad (24)$$

Thus it is natural to define the "minimal" solution of $H(x, p)$ by the opposite of the SDVS of $H(x, -p)$. Obviously, the Hamiltonians $H(x, -p)$ associated with all the SFS Hamiltonians are particular cases of the generic SFS Hamiltonian. Therefore all the previous theoretical and algorithmic results hold for the "minimal" SFS solutions.

The interest of the notion of the "minimal" solution is twofold: first it allows to recover surface which are "globally" concave (whereas SDVSs are "globally" convex). The second interest of these "minimal" solutions lies on a possible extension of the "global algorithm" of Oliensis [40, 17].

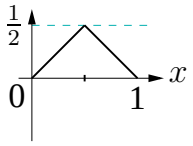

a) solution with H_1

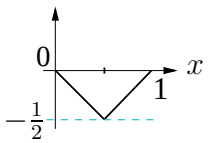

b) solution with $-H_1$

Figure 4: solutions of H versus $-H$; minimal solutions

7 Stability of SDVS and applications to SFS

Now we state a stability result. This stability has important and attractive consequences for the Shape From Shading problem. We consider for $n \in \mathbb{N}$ the equations:

$$H_n(x, \nabla u) = 0, \quad \forall x \in \Omega \quad (25)$$

with continuous, convex and coercive Hamiltonians H_n satisfying the same assumptions as H. We set for any $x \in \overline{\Omega}$:

$$\mathcal{Z}_n(x) = \{p \in \mathbb{R}^N \mid H_n(x, p) \leq 0\},$$

$$\mathcal{S}_n = \{x \in \overline{\Omega} \mid H_n(x, \nabla\psi(x)) = 0\}.$$

We require the following conditions:

$*$ There exists $M > 0$ such that
$$\mathcal{Z}_n(x) \subset B(0, M), \ \forall x \in \overline{\Omega}, n \in \mathbb{N}; \quad (26)$$
$*$ $\theta_n \mathcal{Z}(x) + (1 - \theta_n)\nabla\psi(x) \subset \mathcal{Z}_n(x)$,
for any $x \in \overline{\Omega}$, $n \in \mathbb{N}$; (27)
$*$ $H(x, p) \leq \liminf_{n\to+\infty}{}_* H_n(x, p)$,
for any $(x, p) \in \overline{\Omega} \times B(0, M)$; (28)

where θ_n is a sequence converging toward 1. Above, we have denoted

$$\liminf_{n\to+\infty}{}_* H_n(x,p) \doteq \inf\{\liminf_n H_n(x_n, p_n) : (x_n, p_n) \to (x, p)\}. \quad (29)$$

Theorem 4 (Stability) *Let $u_n : \overline{\Omega} \to \mathbb{R}$ be a sequence of SDVS of* (25)-(6) *on $\overline{\Omega}$. Assume that* (26)-(28) *are satisfied. If u is the SDVS of* (2)-(6)*, then*

$$u(x) = \lim_{n\to\infty} u_n(x)$$

uniformly in $\overline{\Omega}$.

In computer vision, the images are always corrupted by noise. It is therefore very important to design schemes and algorithms *robust* to noise. That is, the result obtained from a noisy images should be close to the ideal result from the perfect image. Moreover, the computer vision algorithms use frequently various parameters. In this work, we assume that the camera is calibrated and that the position of the light source is known. So, for applying our algorithms, the user must input (as parameters) the focal length, the size of the pixels (width, height) and a vector representing the light source direction (following the chosen modeling). In practice, this additional data can be not known precisely and the inputs provided by the

user can contain important errors. Consequently, to be applicable, the algorithms must be robust to these unavoidable errors on parameters. In other words, the returned results by the algorithms with corrupted parameters must be close to the results returned with the perfect theoretical parameters.

Mathematically, the robustness is expressed by the continuity of the application which from an image I (a focal length f or a light source direction $\mathbf{L}$,..., respectively), returns the solution u of the associated PDE. In other words, we would like that, for all sequences of noisy images I_n (of focal lengths f_n or of light source directions $\mathbf{L}_n$,..., respectively) converging toward an image I (f or $\mathbf{L}$,..., respectively), the sequence of recovered solutions u_n converges toward the solution u associated to I (f or $\mathbf{L}$, respectively). If we denote H_n the Hamiltonian obtained by replacing the parameters $\mathbf{L}, \mathsf{f}$ and I by $\mathbf{L}_n, \mathsf{f}_n$ and I_n in H, then the desired stability property corresponds with the convergence of the SDVSs of (25)-(6) towards the SDVS of (2)-(6) when $n \to +\infty$. In lots of cases, Theorem 4 allows to demonstrate that this property is satisfied.

In the sequel, we propose a way allowing to use Theorem 4 and to prove that such results hold for the Shape From Shading problem. We consider the case where $\mathbf{L}_n$ and f_n converge toward $\mathbf{L}$ and f while we fix $I_n = I$ (the case in which also I varies is studied in some situations in the report [43]). Up to a change of variables, we can assume that $\psi \equiv 0$. Our aim is to verify assumptions (26)-(28).

Let us recall that the classical SFS Hamiltonians are special cases of the generic SFS Hamiltonian (see Section 2)

$$H_g(x,p) = \kappa_x \sqrt{|\mathbf{A}_x p + \mathbf{v}_x|^2 + K_x^2} + \mathbf{w}_x \cdot p + c_x$$

where $\kappa_x, \mathbf{A}_x, \mathbf{v}_x, K_x, \mathbf{w}_x$ and c_x are completely described in [48, 42]. For all the SFS Hamiltonians, the functions $\kappa_x, \mathbf{A}_x, \mathbf{v}_x, K_x, \mathbf{w}_x$ and c_x depend continuously on $x, \mathbf{L}$ and f. Let us denote by $\kappa_x^n, \mathbf{A}_x^n, \mathbf{v}_x^n, K_x^n, \mathbf{w}_x^n, c_x^n$ the approximations of $\kappa_x, \mathbf{A}_x, \mathbf{v}_x, K_x, \mathbf{w}_x, c_x$ obtained by replacing $\mathbf{L}$ and f by $\mathbf{L}_n, \mathsf{f}_n$ and H_g^n the corresponding approximation of H_g.

Proposition 2 *If H_g is coercive, then H_g^n is coercive for n sufficiently large and therefore* (26) *is verified.*

PROOF. Let us remind that the coercivity of the SFS Hamiltonians corresponds to assume that there exists $\delta > 0$ such that

$$\kappa_x - |{}^t\mathbf{A}_x^{-1}\mathbf{w}_x| > \delta \text{ for any } x \in \overline{\Omega}$$

(see [48, 42]). Since $\mathbf{L}_n \to \mathbf{L}$ and $\mathsf{f}_n \to \mathsf{f}$ then for n large enough, we have

$$\forall x \in \overline{\Omega}, \quad \kappa_x^n - \left|({}^t\mathbf{A}_x^n)^{-1}\mathbf{w}_x^n\right| > \frac{\delta}{2}$$

so, the functions H_g^n are coercive in p uniformly with respect to $x \in \overline{\Omega}$. In particular, the hypothesis (26) holds. □

For all $x \in \overline{\Omega}$ and $p \in S^1$ (the unit sphere in $\mathbb{R}^2$), let us consider $g : \Omega \times \mathbb{R}^+ \to \mathbb{R}$ defined by

$$g(x,r) = H_g(x, \nabla\psi + rp)$$

and g_n the approximation of g designed from H_g^n. Clearly, there exist $a(x,p)$, $b(x,p)$, $c(x,p)$, $\mu(x,p)$ and $\nu(x,p)$ in $\mathbb{R}$ such that

$$g(x,r,p) = \kappa_x \sqrt{a(x,p)r^2 + b(x,p)r + c(x,p)} + \mu(x,p)r + \nu(x,p). \quad (30)$$

and we have a similar expression for g_n with a_n , b_n, c_n, μ_n and ν_n which are the appropriate approximations. The uniform coercivity of the functions H_g^n and H_g involves that there exists $\delta > 0$ such that $\forall x \in \overline{\Omega}, p \in S^1, n \in \mathbb{N}$,

$$(\kappa_x^n)^2\, a_n(x,p) - \mu_n(x,p)^2 > \delta \quad \text{and} \quad \kappa_x^2 a(x,p) - \mu(x,p)^2 > \delta.$$

Since $\psi \equiv 0$ is a subsolution, we have

$$(\kappa_x^n)^2 c_n(x,p) - \nu_n(x,p)^2 \leq 0 \quad \text{and} \quad \kappa_x^2 c(x,p) - \nu(x,p)^2 \leq 0$$

with a strict inequality outside of $\mathcal{S}$ (recall that since $I_n = I$ then $\mathcal{S}_n = \mathcal{S}$). Note also that ν and ν_n are non positive.
So, by using the Appendix of [42], we can claim that for $x \notin \mathcal{S}$ and $p \in \mathbb{R}^N$, the equation $g(x,r,p) = 0$ has an unique solution in $\mathbb{R}^+$ [5],

[5] Let us fix x in $\overline{\Omega} \setminus \mathcal{S}$. For all our SFS Hamiltonians we have $\psi(x) = argmin_p H(x,p)$ and $H(x, \nabla\psi(x)) < 0$. So, by continuity, coercivity and convexity of H, for all $p \neq 0$, the equation (in $r \in \mathbb{R}$) $H(x, \nabla\psi + rp) = 0$ has two solutions: a positive one and a negative one.

given by:

$$r(x,p) = \frac{-\left(\kappa_x^2 b(x,p) - 2\mu(x,p)\nu(x,p)\right) + \sqrt{\Delta(x,p)}}{2\left(\kappa_x^2 a(x,p) - \mu(x,p)^2\right)}$$

where

$$\Delta(x,p) = \left(\kappa_x^2 b(x,p) - 2\mu(x,p)\nu(x,p)\right)^2 - 4\left(\kappa_x^2 c(x,p) - \nu(x,p)^2\right)\left(\kappa_x^2 a(x,p) - \mu(x,p)^2\right).$$

and the same result holds for the equation $g_n(x,r,p) = 0$. We denote $r_n(x,p)$ its solution and, by using the adequate approximations, we obtain an expression similar to the one of $r(x,p)$. For all $x \in \overline{\Omega} \setminus \mathcal{S}$ and $p \in S^1$, let us denote

$$\theta_n(x,p) = \frac{r_n(x,p)}{r(x,p)}.$$

If (x,p) is fixed in $(\overline{\Omega} \setminus \mathcal{S}) \times S^1$, then we have $\theta_n(x,p) \to 1$, when $n \to +\infty$.

Proposition 3 *If $\theta_n(x,p) \to 1$, uniformly in $x \in \overline{\Omega} \setminus \mathcal{S}$ and $p \in S^1$, then assumption* (27) *holds.*

PROOF. Let us denote by

$$\underline{\theta_n} = \min_{(x,p) \in \overline{\Omega} \setminus \mathcal{S} \times S^1} \theta_n(x,p),$$

we have $\underline{\theta_n} \to 1$ when $n \to +\infty$. In other respects, by hypothesis (3), we have that for any $x \in \overline{\Omega}$ and $q \in \mathcal{Z}(x)$, there exists $\mu \geq 1$ such that

$$\mu q \in \partial \mathcal{Z}(x).$$

By definition of $\theta_n(x,p)$, we have

$$\theta_n\left(x, \frac{q}{|q|}\right)(\mu q) \in \partial \mathcal{Z}_n(x).$$

Since $0 \leq \underline{\theta_n} \leq \mu \theta_n\left(x, \frac{q}{|q|}\right)$, the hypothesis (3) involves

$$\underline{\theta_n} q \in \mathcal{Z}_n(x).$$

Thus, we have proved that for any $x \in \overline{\Omega}$,

$$\underline{\theta_n} \mathcal{Z}(x) \subset \mathcal{Z}_n(x).$$

and therefore hypothesis (27) holds. □

Since (28) clearly holds, we can apply Theorem 4 to get the stability statement.

We now give an examples for which $\theta_n(x,p) \to 1$, uniformly. Unfortunately, we have not found a generic proof. Note that the difficulty is in a neighborhood of $\mathcal{S}$ where $r(x,p)$ and $r_n(x,p)$ get arbitrarily small.

EXAMPLE : Let us consider the example of the Hamiltonian $H_{D/O}^{orth}$ with $\mathbf{L}_n \to \mathbf{L}$. So

$$H(x,p) = I(x)\sqrt{1 + |p|^2 - 2p \cdot \mathbf{l}} + p \cdot \mathbf{l} - 1$$

and

$$H_n(x,p) = I(x)\sqrt{1 + |p|^2 - 2p \cdot \mathbf{l}_n} + p \cdot \mathbf{l}_n - 1.$$

Easily, one can verify that

$$r(x,p) = \sqrt{1 - I(x)^2}\frac{I(x)\sqrt{1 - (p \cdot \mathbf{l})^2} - (p \cdot \mathbf{l})\sqrt{1 - I(x)^2}}{I(x)^2 - (p \cdot \mathbf{l})^2},$$

and that for any $x \in \overline{\Omega}$, $p \in S^1$,

$$\theta_n(x,p) = \frac{I(x)\sqrt{1 - (p \cdot \mathbf{l}_n)^2} - (p \cdot \mathbf{l}_n)\sqrt{1 - I(x)^2}}{I(x)\sqrt{1 - (p \cdot \mathbf{l})^2} - (p \cdot \mathbf{l})\sqrt{1 - I(x)^2}} \cdot \frac{I(x)^2 - (p \cdot \mathbf{l})^2}{I(x)^2 - (p \cdot \mathbf{l}_n)^2}.$$

We claim that if the brightness image I is Lipschitz-continuous on $\overline{\Omega}$, then $\partial_x \theta_n(x,p)$ is bounded independently of $x \in \overline{\Omega}$, $n \in \mathbb{N}$ and p on a neighborhood of S^1.

To prove the claim, denote $s_n = p \cdot \mathbf{l}_n$ and $s = p \cdot \mathbf{l}$.

Note that $s_n \to s$ uniformly with respect to p in a neighborhood of S^1. Let us consider the function $T : \mathbb{R} \to \mathbb{R}$ defined by

$$T(X) = \frac{\sqrt{1 - s_n}X - s_n\sqrt{1 - X^2}}{\sqrt{1 - s}X - s\sqrt{1 - X^2}}.$$

For $\delta > 0$ (and small enough), we have for all n large enough, $|s_n| < |s| + \delta \leq 1$, T is continuously derivable on $[s + \delta, 1]$ and T' is bounded independently of s_n[6].

By the uniform coercivity assumption, there exists

[6] so independently of n and p in a neighborhood of S^1.

$\delta > 0$ such that for all p in a neighborhood of S^1 and for all n large enough,

$$|s_n| < |s| + \delta < \min_{x \in \overline{\Omega}} I(x) \leq 1.$$

Since,

$$\nabla_x (T \circ I)(x) = T'(I(x)) \nabla_x I(x),$$

therefore $\nabla_x (T \circ I)$ is bounded independently of x, p and n. We can conclude by using the fact that the function

$$x \mapsto \frac{I(x)^2 - (p \cdot \mathbf{l})^2}{I(x)^2 - (p \cdot \mathbf{l}_n)^2}$$

and its gradient is bounded independently of x in $\overline{\Omega}$, n in $\mathbb{N}$ and p in a neighborhood of S^1.

In a same way, we prove that $\partial_p \theta_n(x,p)$ is uniformly bounded. Let us denote $X = (x,p)$. So we have $\nabla_X \theta_n(X)$ uniformly bounded. Moreover, $\forall X, Y \in \overline{\Omega} \times S^1$,

$$|\theta_n(X) - \theta_n(Y)| \leq |\nabla_X \theta_n|_\infty d(X,Y),$$

where $d(X,Y)$ is the Euclidean geodesic distance in $\Omega \times S^1$. Also, it is well known [33] that for any fixed $X \in \overline{\Omega}$, $Y \mapsto d(X,Y)$ is *Lipschitz continuous* in $\overline{\Omega} \times S^1$ and that the Lipschitz constant does not depend with respect to X. Thus the functions θ_n are uniformly Lipschitz continuous. Therefore the convergence of the sequence θ_n is uniform.

8 Numerical approximation of the SDVS for generic SFS

This section explains how to compute a numerical approximation of the SDVS of the generic SFS equation. This requires three steps. First we "regularize" the equation. Second, we approximate the "regularized" SFS equation by approximation schemes. Finally, by the approximation schemes, we design numerical algorithms.

8.1 Regularization of the equation

The first step of the approximation scheme is a regularization of the equation obtained by cutting the image intensity at a certain level strictly less than 1 before applying the approximation procedure. Given a continuous image I and $n \in \mathbb{N}$, we set

$$I_n(x) = \min\left(I(x), 1 - \frac{1}{n}\right), \quad x \in \overline{\Omega}.$$

As a consequence of Theorem 4 (see [42, 43]), it is possible to show that, if u_n denote the solution of (2)-(6) with the Hamiltonian H_n obtained replacing $I(x)$ by $I_n(x)$ in H, then u_n converges toward the unique singular viscosity solution of (2)-(6).
Now, let us remark that, for any n, the SFS Hamiltonian H_n is not degenerate anymore (i.e $\mathcal{S}_n = \emptyset$). So, its (unique) singular viscosity solution is the (unique) discontinuous viscosity solution. Thus from now we consider the case of an image intensity strictly less than 1 and therefore, for approximating the corresponding equation, we can use the classical tools we have developed in [48].

8.2 Management of the state constraints

In this section, we explain how to deal with the state constraints *in practice*. In particular, we show that, in the setup of this paper, the state constraints can always be rewritten as a Dirichlet boundary condition.
Let u be the SDVS of equation (2)-(6):

$$\begin{cases} H(x, \nabla u) = 0 & \forall x \in \Omega, \\ u(x) = \varphi(x) & \forall x \in \partial\Omega \cup \mathcal{S} \end{cases}$$

In section 3, we have seen that u is Lipschitz continuous and then bounded on Ω. Let $M \in \mathbb{R}$ an upper bound of u on Ω such that

$$\forall x \in \Omega, \quad u(x) < M - 1.$$

Now, let us consider $\tilde{\varphi}$ the real function defined on $\partial\Omega \cup \mathcal{S}$ by

$$\tilde{\varphi}(x) = \min(M, \varphi(x)),$$

and let $\tilde{u}$ be the SDVS of equation

$$\begin{cases} H(x, \nabla u) = 0 & \forall x \in \Omega, \\ u(x) = \tilde{\varphi}(x) & \forall x \in \partial\Omega \cup \mathcal{S}. \end{cases}$$

Following these notations, we have

Proposition 4 *$\tilde{u}$ and u coincide on Ω, i.e.*

$$\forall x \in \Omega, \qquad \tilde{u}(x) = u(x).$$

PROOF. We refer the interested reader to our technical report [43]. □

Therefore, equations (2)-(6) with some state constraints (i.e. such that for some $x \in \partial\Omega \cup \mathcal{S}$ $\varphi(x) = +\infty$) can rewritten as equations without state contraints; i.e with (finite) Dirichlet boundary conditions on the whole set $\partial\Omega \cup \mathcal{S}$. So in practice, we always consider (finite) Dirichlet boundary conditions: when we know the values of the solution on $\partial\Omega$ we can transfer these informations in φ; when we do not have this data and we want to compute the solution of with state contraints, we impose φ to be a "great" *constant* (in practice in our C++ code, we have chosen the constant `FLT_MAX`). Let us emphasize that by modifying φ in such a way, we do not change the solution of (2)-(6) neither the approximation computed by our algorithm.

8.3 Approximation schemes and numerical algorithms for the generic SFS problem

In [48, 45, 47], we have designed SFS monotonous approximation schemes which are always stable (we say that a scheme $S(\rho, x, u(x), u) = 0$ is stable[7] if for all fixed mesh size ρ it has solutions and if all the solutions are bounded independently of ρ). Moreover, we also prove in [48, 45, 42] that (as soon as the intensity image is Lipschitz continuous and the Hamiltonian is coercive) the solutions of these schemes converge toward the viscosity solution of the adequate SFS equation when the mesh size vanishes. For each scheme described in [48, 45], we design (in [48, 45]) an algorithm that computes some numerical approximations of a solution u^ρ of the considered scheme. Moreover, we prove that the computed numerical approximations converge toward u^ρ. In the sequel of this section, we quickly remind our numerical method.

The reader unfamiliar with the notion of approximation schemes can refer to [3] or [42]. Let us just recall that, following [3], an approximation scheme is a functional equation of the form

$$S(\rho, x, u(x), u) = 0 \qquad \forall x \in \overline{\Omega},$$

which "approximates" the considered PDE. S is defined on $\mathcal{M} \times \overline{\Omega} \times \mathbb{R} \times B(\overline{\Omega})$ into $\mathbb{R}$, $\mathcal{M} = \mathbb{R}^+ \times \mathbb{R}^+$ and $\rho = (h_1, h_2) \in \mathcal{M}$ defines the size of the mesh that is used in the corresponding numerical algorithms. $B(D)$ is the space of bounded functions defined on a set D. For ensuring the stability of a scheme, it is globally sufficient that it is monotonous (i.e. the function $u \mapsto S(\rho, x, t, u)$ is nonincreasing) and that the function $t \mapsto S(\rho, x, t, u)$ is nondecreasing, see [48, 45]. For obtaining such a scheme, we approximate the generic Hamiltonian H_g by

$$H_g(x, \nabla u(x)) \approx \sup_{a \in \overline{B}(0,1)} \{ \sum_{i=1}^{2} (-f_i(x,a)) \frac{u(x) - u(x + s_i(x,a) h_i \vec{e_i})}{-s_i(x,a) h_i} - l_g(x,a) \}$$

where $f_i(x,a)$ is the i^{th} component of $f_g(x,a)$ and $s_i(x,a)$ is its sign (see [48, 45]). Thus, we obtain the approximation scheme $S_{impl}(\rho, x, u(x), u) = 0$ with S_{impl} defined by:

$$S_{impl}(\rho, x, t, u) = \sup_{a \in \overline{B}(0,1)} \{ \sum_{i=1}^{2} (-f_i(x,a)) \frac{t - u(x + s_i(x,a) h_i \vec{e_i})}{-s_i(x,a) h_i} - l_g(x,a) \}.$$

By introducing a fictitious time $\Delta\tau$, we also transform this implicit scheme in a "semi-implicit" scheme (also monotonous):

$$S_{semi}(\rho, x, t, u) = t - (u(x) + \Delta\tau \, S_{impl}(\rho, x, u(x), u)),$$

where $\Delta\tau = (f_g(x, a_0) \cdot (1/\Delta x_1 1, 1/\Delta x_1 2))^{-1}$; a_0 being the optimal control associated with $S_{impl}(\rho, x, u(x), u)$. Let us emphasize that these two schemes have exactly the same solutions and that they verify the previous monotonicity conditions (with respect to t and u). Thus, we can prove (see [48, 42, 45]) the stability of these two schemes.

By construction, these two schemes are consistent[7] with the SFS equations as soon as the brightness image I is Lipschitz continuous; see [48, 42, 45]. Using the stability and the monotonicity of the schemes and some uniqueness results, it follows directly from [3] that the solutions of the approximation schemes S_{impl} and S_{semi} converge towards the viscosity solution

[7] Following Barles and Souganidis definitions [3].

of the considered equation (complemented with the adequate boundary conditions) when the mesh size vanishes; see [48, 42, 45].

We now describe an *iterative algorithm* that computes numerical approximations of the solutions of a scheme $S(\rho, x, u(x), u) = 0$ for all fixed $\rho = (h_1, h_2)$. We denote, for $k \in \mathbb{Z}^2$, $x_k = (k_1 h_1, k_2 h_2)$, and $Q := \{k \in \mathbb{Z}^2 \text{ s.t. } x_k \in \overline{\Omega}\}$. We call "pixel" a point x_k in $\overline{\Omega}$. Since $\overline{\Omega}$ is bounded the number of pixels is finite. The following algorithm computes for all $k \in Q$ a sequence of approximations U_k^n of $u(x_k)$:

Algorithm:

1. *Initialisation ($n = 0$): $\forall k \in Q$, $U_k^0 = u_0(x_k)$;*
2. *Choice of a pixel x_k and modification (step $n+1$) of U_k^n: we choose U^{n+1} such that*

$$\begin{cases} U_l^{n+1} = U_l^n \quad \text{if} \quad l \neq k, \\ S(\rho, x_k, U_k^{n+1}, U^n) = 0; \end{cases}$$

3. *Choose the next pixel x_k (using alternating raster scans [15]) and go back to 2.*

In [45], we prove that if u_0 is a supersolution of the SFS scheme S_{impl} (respectively, S_{semi}) then step 2 of the algorithm has always an unique solution and that the computed numerical solutions converge (when $n \to +\infty$) toward the solutions of the scheme. Many details about the implementation of the algorithms can be found in [48, 42, 45].

8.4 Examples of SFS results obtained from synthetic images

Let us recall that our method does not necessarily require boundary data. Figure 5 shows some reconstructions of the Mozart face when using the exact boundary data on the boundary of the image and at all critical points (Fig.5-c), when using the exact boundary data at all the critical points and state constraints on the boundary of the image (Fig.5-d), and with no boundary data, except for the tip of the nose (Fig.5-e). Let us remark that, as the theory predicted, our algorithms show an exceptional robustness to noise and errors on the parameters; This robustness is even bigger when we send the boundary to infinity (apply the state constraints). Figure 6 displays a reconstruction of Mozart's face from an image perturbed by additive uniformly distributed white noise (SNR $\simeq 5$) by using the implicit algorithm (see [45]) with the wrong parameters $\mathbf{l}_\varepsilon = (0.2, -0.1)$ and $\mathsf{f}_\varepsilon = 10.5$ (focal length) and without any boundary data. The original image Fig.6-a) has been synthesized with $\mathbf{l} = (0.1, -0.3)$ and $\mathsf{f} = 3.5$. The angle between the initial light vector $\mathbf{L}$ and the corrupted light vector $\mathbf{L}_\varepsilon$ is around 13°.

9 Toward applications of Shape From Shading

In this section, we suggest some *applications* of our SFS method. We do not provide complete descriptions, but we hope that the results will convince the reader of the *applicability of our SFS method to real problems*. Let us emphasize that all the results we present in this section are obtained from *real images*:

Note: When we apply SFS methods to real images we assume that the camera is geometrically and photometrically calibrated. In our experiments of sections 9.1 and 9.2 we know the focal length (5.8 mm) and approximately the pixel size (0.0045 mm; CCD size = 1/2.7") of our cheap digital camera (Pentax Optio 330GS). In section 9.3, we choose some arbitrary reasonable parameters. Also, note that there exist classical methods to calibrate photometrically a camera [35, 36]. In our tests, we do not use them, but we make some educated guesses for gamma correction (when the photometric properties of the images seem incorrect).

9.1 Document restoration using SFS

In this section, we propose a *reprographic system*[8] to remove the geometric and photometric distortions generated by the classical photocopy of a bulky book. A first solution has been proposed by Wada and coworkers [58] who deal with *scanner* images involving a complex optical system (with a moving light). Here, the acquisition process we use is a classical camera (a camera snapshot is practically instantaneous, whereas a scan takes several seconds). The book is illuminated by a single light source located at infinity or close

[8] Suggested to us by Durou (private communication); see [13].

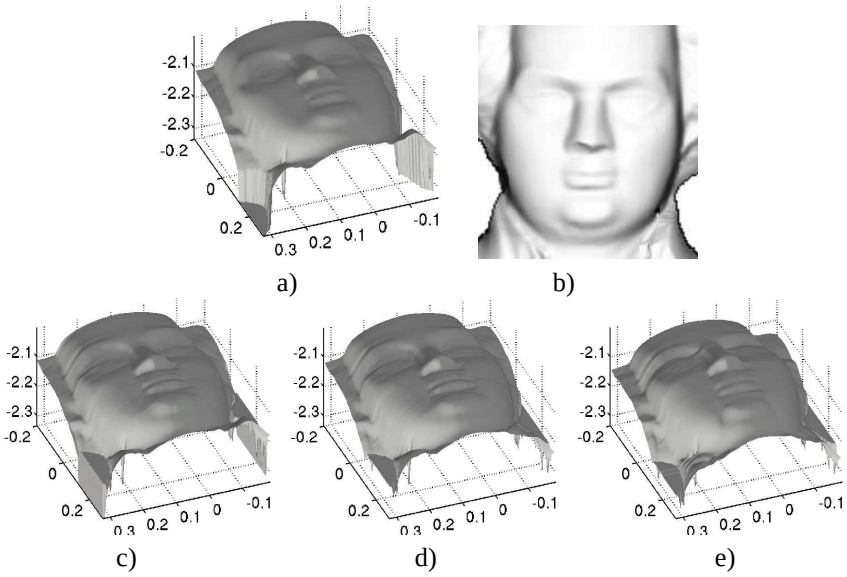

Figure 5: Reconstruction of Mozart's face *with and without* boundary data.
a) original surface; b) image generated from a) [size $\simeq 200 \times 200$]; c) reconstructed surface from b) with the implicit algorithm (IA) after only 3 iterations, using the exact boundary data on the boundary of the image and at all critical points: $\varepsilon_1 \simeq 0.56$, $\varepsilon_2 \simeq 0.0018$, $\varepsilon_\infty \simeq 0.42$; d) reconstructed surface by the IA (after 3 iterations) with state constraints on the boundary of the image: $\varepsilon_1 \simeq 0.58$, $\varepsilon_2 \simeq 0.0019$, $\varepsilon_\infty \simeq 0.42$; e) reconstructed surface by the IA (after 3 iterations) with state constraints on the boundary of the image and at all the critical points except at the one on the nose: $\varepsilon_1 \simeq 0.60$, $\varepsilon_2 \simeq 0.0020$, $\varepsilon_\infty \simeq 0.42$.

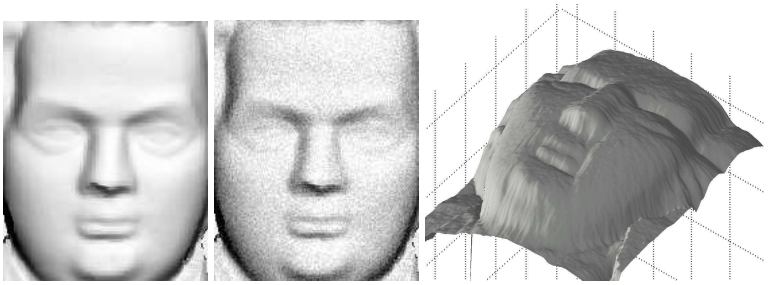

Figure 6: Reconstruction of Mozart's face from a noisy image with the wrong parameters $\mathbf{l}_\varepsilon = (0.2, -0.1)$ and $\mathsf{f}_\varepsilon = 10.5$.
a) Image generated from Mozart's face represented in Fig.5-a) with $\mathbf{l} = (0.1, -0.3)$ and $\mathsf{f} = 3.5$ [size $\simeq 200 \times 200$]; b) noisy image (SNR $\simeq 5$); c) reconstructed surface from b) after 4 iterations of the implicit algorithm, using the incorrect parameters $\mathbf{l}_\varepsilon = (0.2, -0.1)$ and $\mathsf{f}_\varepsilon = 10.5$, and with state constraints on the boundary of the image and at all the critical points except at the critical point on the nose.

to the optical center (following the models we describe in section 2). Note that Cho et al. [11] propose a similar system but they use two light sources[9]. The acquired images are then processed using our SFS method to obtain the shape of the photographed page. Let us emphasize that, for obtaining a compact experimental system, the camera must be located relatively close to the book. Therefore the *perspective model is especially relevant* for this application. Also, the distortion due to the perspective clearly appears in the image a) of Figure 9.

In our SFS method we assume that the albedo is constant. In this application, this does not hold because of the printed parts. Before recovering the surface of the page, we therefore localize the printed parts by using image statistic (similar to Cho's [11])[10] and we erase them automatically by using e.g. the inpainting algorithm of Tschumperlé and Deriche [57]. This step can produce an important pixel noise. Nevertheless, this is not a problem for us because, as Figure 8-b) shows, *our SFS method is extremely robust to pixel noise*: Figure 8-b) displays the result produced by our algorithm (after 10 iterations) using the image of a text page with its pigmented parts, Fig.8-a). In this test, characters are considered as noise. Note that one could say that such a restoration system (based on SFS) is flawed because it does not use the information provided by the *rows* of characters. This is partially true but nevertheless, for pages containing few rows of characters but a lot of graphics and pictures (separated by large white bands as it is often the case for scientific documents), such a SFS method could provide a simple and efficient solutions.

Once we have recovered the three-dimensional shape of the page, we can flatten the surface by using e.g. the algorithm of Brown and Seales [5]. Note that at each step of this restoration process (3D reconstruction and flattening) we keep the correspondences with the pixels in the image. Thus, at the final step, we can restore the printed parts.

To prove the applicability of this method, we have tested it on a page mapped on a cylindric surface (we have used our cheap camera and flash in an approximately dark room). Figure 9 shows the original image in a), the reconstructed surface (after 10 iterations) (textured by the ink parts of a)) in b) and an orthographic projection of the reconstructed surface, in c). Figure 9-c) indicates that our method allows to remove the perspective and photometric distortions.

[9] We can also note that the numerical method proposed by [11] requires that global variations of depth only exist along one direction. Our method does not require this hypothesis.

[10] Most probably, we can also achieve this step by using the excellent work of Bell and Freeman [4] who propose a learning-based approach.

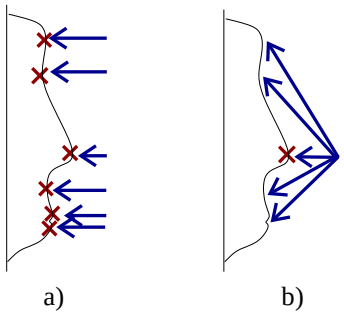

Figure 7: Critical points of the profile of a face. a) Critical points (6) for a homogeneous horizontal light; b) Critical point for a point light source at the optical center.

9.2 Face reconstruction from SFS

The interest of the SFS methods for some applications dealing with faces has been demonstrated in e.g. the work of Zhao and Chellappa [62] (who use symmetric SFS for illumination-insensitive face recognition), by Smith and Hancock [51] (who use SFS needle map for face recognition), and by Choi and coworkers [12] (who use SFS for determining the face pose). In this section we propose a very simple protocol based on SFS for face reconstruction. We use one camera equipped with a basic flash in an approximately dark place. As shown in Figure 7, the interest of this method lies in the fact that, with such a protocol, the generated image should contain an unique critical point (if the distance of the face to the camera and the focal length are sufficiently small). Therefore, the propagation of the height information starts from this unique critical point.

We have tested our generic algorithm on a real image of a face (slightly made-up to be more Lambertian) located at $\simeq$700 mm of the camera in an approximately dark place (see Fig.10-a)). Figure

10-b) shows the surfaces recovered by our generic algorithm (after 5 iterations) with the perspective SFS model with a point light source at the optical center. As in the previous application, the albedo is not constant over the whole image. Therefore we removed the eyes and the eyebrows in the image by using e.g. the inpaiting algorithm of Tschumperlé and Deriche [57]. Moreover, note that this step can be automated by matching the image to a model image already segmented (we can use for example the very robust multi-modal and non-rigid matching method proposed by Hermosillo and Faugeras in [24]). Figure 10 shows in c) the surface recovered from the image obtained after the inpainting process.

9.3 Potential applications to medical images

In this section, we are interested in applying our SFS method to some medical images. Our interest is motivated by the work of Craine et al. [14], Okatani and Deguchi [37], Forster and Tozzi [23], Smithwick and Seibel [52], Yeung et al. [60], Gillies et al. [54, 32] and Yamany et al. [59]. For illustrating the relevance of the "perspective SFS" modeling with the light source located at infinity, we apply our algorithm to an endoscopic image of a normal stomach[11] (see Figure 11-a)). In fact, for producing such an image, the light source must be very close to the camera, because of space constraints. In Figure 11-b), we show the result obtained (after 3 iterations) by our generic algorithm in the perspective case with the light source at the optical center. In Figure 11-b), the surface is visualized with a light source located at the optical center. This reconstruction looks quite good. To further show the quality of the reconstruction, we display in c), the surface b) with a different illumination. Finally, notice that the stomach wall is not perfectly Lambertian (see Fig.11-a)). This suggests the robustness of our SFS method to departures from the Lambertian hypothesis.

[11] Suggested by Tankus and Sochen (private communication,[56]) and downloaded from http://www.gastrolab.net/.

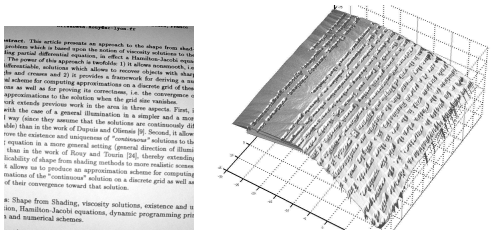

a) b)

Figure 8: a) Real image of a page of text [size $\simeq 800 \times 800$]; b) Surface recovered from a) by our generic algorithm (without removing the printed parts of a)).

10 Conclusion

We have developed a new mathematical framework which unifies various SFS theories (in particular, it unifies the work of Lions et al. [34, 50], of Dupuis and Oliensis [17], of Falcone et al. [7, 21] and of Prados and Faugeras [49, 46]) and generalizes them to all SFS Hamiltonians, (in particular, we generalize them to "perspective SFS" with a light source located at the infinity or at the optical center). The class of weak solutions we have defined in this paper is really more adapted to the SFS specifications than the other classical notions used in [34, 50, 7, 21, 49, 46]; in particular, it does not necessarily require boundary data. Finally, we have successfully applied our SFS method to real images and we have suggested that it may be useful in a number of real-life applications.

References

[1] M. Bardi and I. Capuzzo-Dolcetta. *Optimal control and viscosity solutions of Hamilton-Jacobi-Bellman equations*. Birkhauser, 1997.

[2] G. Barles. *Solutions de Viscosité des Equations de Hamilton–Jacobi*. Springer–Verlag, 1994.

[3] G. Barles and P.E. Souganidis. Convergence of approximation schemes for fully nonlinear second order equations. *Asymptotic Analysis*, 4:271–283, 1991.

[4] M. Bell and W.T. Freeman. Learning local evidence for shading and reflectance. In *Proceedings of the International Conference on Computer Vision (ICCV'01)*, volume 1, pages 670–677, July 2001.

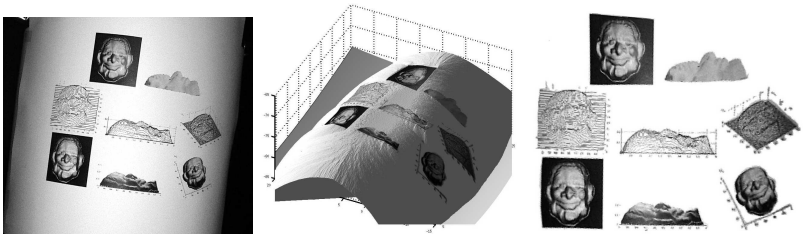

a) b) c)

Figure 9: a) real image of a page containing pictures and graphics [size $\simeq 2000 \times 1500$], b) surface (textured by the printed parts of a)) recovered from a) by our generic algorithm (after having removed and inpainted the ink parts of a)). c) An orthographic projection of the surface b): the geometric (and photometric) distorsions are significantly reduced.

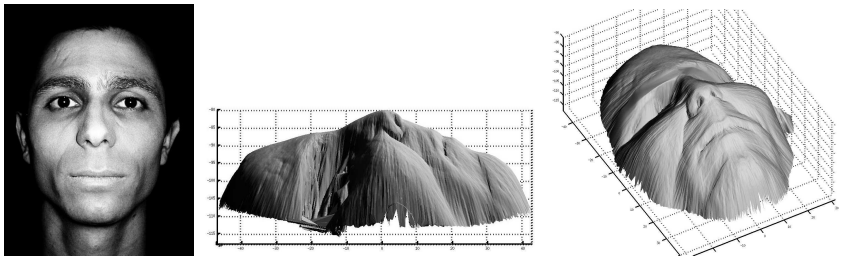

a) b) c)

Figure 10: Face reconstruction from SFS: a) Real face image [size $\simeq 450 \times 600$]; b) surface recovered from a) by our generic algorithm with the perspective model with the light source located at the optical center; c) surface recovered by our generic algorithm with the same modeling hypotheses after the inpainting process.

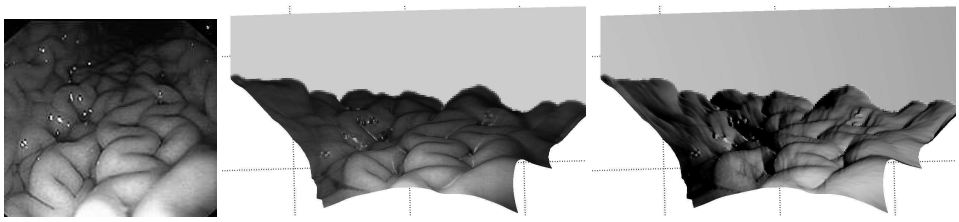

a) b) c)

Figure 11: Reconstruction of a normal stomach: a) Original image of a normal stomach [size$\simeq$ 200×200]; b) surface recovered from a) by our generic algorithm with the perspective model and with the light source located at the optical center; c) surface b) visualized with a different illumination.

[5] M. S. Brown and W. B. Seales. Document restoration using 3D shape. In *ICCV'01*, 2001.

[6] A. M. Bruckstein. On shape fron shading. *Computer Vision Graphics Image Process*, 44:139–154, 1988.

[7] F. Camilli and M. Falcone. An approximation scheme for the maximal solution of the shape-from-shading model. In *ICIP'96*, pages 49–52, 1996.

[8] F. Camilli and A. Siconolfi . Maximal subsolutions for a class of degenerate hamilton-jacobi problems. *Indiana Univ. Math. J.*, 48(3):1111–1132, 1999.

[9] F. Camilli and A. Siconolfi . Nonconvex degenerate Hamilton-Jacobi equations. *Mathematische Zeitschrift*, 242:1–21, 2002.

[10] I. Capuzzo-Dolcetta and P.-L. Lions. Hamilton-jacobi equations with state constraints. *Trans. Amer. Math. Soc.*, 318(2):643–68, 1990.

[11] S.I. Cho and H. Saito. A Divide-and-Conquer Strategy in Shape from Shading problem. In *CVRP'97*. IEEE Computer Society, 1997.

[12] K.N. Choi, P. Worthington, and E.R. Hancock. Facial pose using shape-from-shading. In *BMVC'99*, pages 402–411, 1999.

[13] F. Courteille, A. Crouzil, J-D. Durou, and P. Gurdjos. Towards shape from shading under realistic photographic conditions. In *ICPR'04*, pages 277–280 (volume 2). IAPR, 2004.

[14] B.L. Craine, Craine E.R., C.J. O'Toole, and Q. Ji. Digital imaging colposcopy: Corrected area measurements using Shape-from-Shading. *IEEE Transactions on Medical Imaging*, 17(6):1003–1010, 1998.

[15] P.-E. Danielsson. Euclidean Distance Mapping. *Computer Graphics and Image Processing*, 14(3):227–248, 1980.

[16] P. Dupuis and J. Oliensis. Direct method for reconstructing shape from shading. *SPIE*, 1570:116–128, 1991.

[17] P. Dupuis and J. Oliensis. An optimal control formulation and related numerical methods for a problem in shape reconstruction. *The Annals of Applied Probability*, 4(2):287–346, 1994.

[18] P. Dupuis and J. Oliensis. Shape From Shading: Provably convergent algorithms and uniqueness results. In *ECCV'94*, volume 2, pages 256–268, 1994.

[19] J-D. Durou, M. Falcone, and M. Sagona. A survey of numerical methods for shape from shading. Research report 2004-2-R, IRIT, January 2004.

[20] J.-D. Durou and H. Maître. On convergence in the methods of Strat and Smith for shape from shading. *IJCV*, 17(3):273–289, 1996.

[21] M. Falcone and M. Sagona. An algorithm for the global solution of the shape-from-shading model. *ICIAP*, 1:596–603, 1997. LNCS 1310.

[22] M. Falcone, M. Sagona, and A. Seghini. A scheme for the shape-from-shading model with "black shadows". In *Proceedings of ENUMATH 2001*, 2001.

[23] C.H.Q. Forster and C.L. Tozzi. Towards 3d reconstruction of endoscope images using shape from shading. In *13th Brazilian Symposium on Computer Graphics and Image Processing (SIBGRAPI)*. IEEE Computer Society, October 2000.

[24] G. Hermosillo and O. Faugeras. Dense image matching with global and local statistical criteria: a variational approach. In *Proceedings of CVPR (1)*. IEEE Computer Society, 2001.

[25] B.K. Horn and M.J. Brooks, editors. *Shape from Shading*. The MIT Press, 1989.

[26] B.K.P. Horn. Obtaining shape from shading information. In P.H. Winston, editor, *The Psychology of Computer Vision*. McGraw-Hill, New York, 1975.

[27] H. Ishii and M. Ramaswamy. Uniqueness results for a class of Hamilton-Jacobi equations with singular coeffi cients. *Comm. Par. Diff. Eq.*, 20:2187–2213, 1995.

[28] R. Kimmel and A.M. Bruckstein. "Global shape-from-shading". *CVGIP: Image Understanding*, pages 360–369, 1995.

[29] R. Kimmel and A.M. Bruckstein. Tracking level sets by level sets : A method for solving the shape from shading problem. *Computer Vision and Image Understanding*, 62(2):47–58, 1995.

[30] R. Kimmel and J.A. Sethian. Optimal algorithm for shape from shading and path planning. *JMIV*, 14(2):237–244, 2001.

[31] R. Klette, R. Kozera, and K. Schlüns. Shape from shading and photometric stereo methods. Technical Report CITR-TR-20, University of Auckland, New Zealand, 1998.

[32] C.K. Kwoh, G.N. Khan, and D.F. Gillies. Automated endoscope navigation and advisory system from medical imaging. In *Proceedings of SPIE'99*, volume 3660, 1999.

[33] P.-L. Lions. *Generalized Solutions of Hamilton–Jacobi Equations*. Number 69 in Research Notes in Mathematics. Pitman Advanced Publishing Program, 1982.

[34] P.-L. Lions, E. Rouy, and A. Tourin. Shape-from-shading, viscosity solutions and edges. *Numer. Math.*, 64:323–353, 1993.

[35] C.S. McCamy, H. Marcus, and J.G. Davidson. A colorrendition chart. *J. App. Photog. Eng.*, 2:95–99, 1976.

[36] G.W. Meyer. Wavelength selection for synthetic image generation. *CVGIP*, 41:57–79, 1988.

[37] T. Okatani and K. Deguchi. Shape reconstruction from an endoscope image by shape from shading technique for a point light source at the projection center. *CVIU*, 66(2):119–131, May 1997.

[38] J. Oliensis. Shape from shading as a partially well–constrained problem. *CVGIP: Image Understanding*, 54(2):163–183, 1991.

[39] J. Oliensis. Uniqueness in shape from shading. *IJCV*, 2(6):75–104, 1991.

[40] J. Oliensis and P. Dupuis. A global algorithm for shape from shading. In *Proceedings of ICCV'93*, pages 692–701, 1993.

[41] E. Prados. Une approche du "Shape from Shading" par solutions de viscosit´e. Master's thesis, University of Nice-Sophia Antipolis, France (In French), INRIA, September 2001.

[42] E. Prados. *Application of the theory of the viscosity solutions to the Shape From Shading problem*. PhD thesis, University of Nice-Sophia Antipolis, October 2004.

[43] E. Prados, F. Camilli, and O. Faugeras. A viscosity method for Shape-From-Shading without boundary data. Technical Report RR-5296, INRIA, 2004.

[44] E. Prados, F. Camilli, and O. Faugeras. A viscosity solution method for shape-from-shading without boundary data. *Submitted to ESAIM: Mathematical Modelling and Numerical Analysis*, 2005.

[45] E. Prados and O. Faugeras. A mathematical and algorithmic study of the lambertian SFS problem for orthographic and pinhole cameras. Technical Report RR-5005, INRIA, 2003.

[46] E. Prados and O. Faugeras. "Perspective Shape from Shading" and viscosity solutions. In *Proceedings of ICCV'03*, volume 2, pages 826–831. IEEE Computer Society, 2003.

[47] E. Prados and O. Faugeras. Unifying approaches and removing unrealistic assumptions in Shape from Shading: Mathematics can help. In *Proceedings of ECCV'04 (4)*, volume 3024 of *Lecture Notes in Computer Science*, pages 141–154. Springer, 2004.

[48] E. Prados and O. Faugeras. A generic and provably convergent shape-from-shading method for orthographic and pinhole cameras. *Accepted to The International Journal of Computer Vision*, 2005.

[49] E. Prados, O. Faugeras, and E. Rouy. Shape from shading and viscosity solutions. In *Proceedings of ECCV'02*, volume 2351 of *Lecture Notes in Computer Science*, pages 790–804. Springer, 2002.

[50] E. Rouy and A. Tourin. A Viscosity Solutions Approach to Shape-from-Shading. *SIAM J. of Numerical Analysis*, 29(3):867–884, 1992.

[51] W.A.P. Smith and E.R. Hancock. Face recognition using Shape-from-Shading. In *Proceedings of British Machine Vision Conference (BMVC))*, pages 597–606, September 2002.

[52] Q.Y.L. Smithwick and E.J. Seibel. Depth enhancement using a scanning fiber optical endoscope. In *Proceedings of SPIE BiOS*, 2002.

[53] H. M. Soner. Optimal control with state space constraints. *SIAM J. Contr. Optim*, 24:Part I: 552–562, Part II: 1110–1122, 1986.

[54] L. E. Sucar, D. F. Gillies, and H. Rashid. Integrating shape from shading in a gradient histogram and its application to endoscope navigation. In *Proceedings of 5th International Conference on Artifi cial Intelligence (ICAI-V)*, 1992.

[55] A. Tankus, N. Sochen, and Y. Yeshurun. A new perspective [on] Shape-from-Shading. In *ICCV'03*, volume 2, pages 862–869, 2003.

[56] A. Tankus, N. Sochen, and Y. Yeshurun. Reconstruction of medical images by perspective Shape-from-Shading. In *ICPR'04*, 2004.

[57] D. Tschumperl´e and R. Deriche. Vector-valued image regularization with PDE's : A common framework for different applications. In *CVPR'03*, 2003.

[58] T. Wada, H. Ukida, and T. Matsuyama. Shape from shading with interreflections under proximal light source-3D shape reconstruction of unfolded book surface from a scanner image. In *ICCV'95*, 1995.

[59] S.M. Yamany and A.A. Farag. A system for human jaw modeling using intra-oral images. In *IEEE-EMBS*, volume 20, pages 563–566, 1998.

[60] S.Y. Yeung, H.T. Tsui, and A. Yim. Global shape from shading for an endoscope image. In Chris Taylor and Alan C. F. Colchester, editors, *Proceedings of Medical Image Computing and Computer-Assisted Intervention (MICCAI)*, volume 1679 of *Lecture Notes in Computer Science*, pages 318–327, September 1999.

[61] R. Zhang, P.-S. Tsai, J.-E. Cryer, and M. Shah. Shape from Shading: A survey. *IEEE Transactions on Pattern Analysis and Machine Intelligence*, 21(8):690–706, August 1999.

[62] W. Zhao and R. Chellappa. Illumination-insensitive face recognition using symmetric Shape-from-Shading. In *CVPR'00*, pages 1286–1293, 2000.